DOI: 10.1021/ma102065u

Macromolecules
ARTICLE

Surface-Grafted Polymers from Electropolymerized Polythiophene RAFT Agent

Carlos D. Grande, Maria Celeste Tria, Guoqian Jiang, Ramakrishna Ponnapati, and Rigoberto Advincula*

Department of Chemistry and Department of Chemical and Biomolecular Engineering, University of Houston, Houston, Texas 77204-5003, United States

Received September 6, 2010; Revised Manuscript Received December 17, 2010

ABSTRACT: The synthesis of grafted homopolymer and block copolymer films is reported using a surface-initiated reversible addition−fragmentation chain transfer (SI-RAFT) polymerization from electropolymerized polythiophene on indium tin oxide (ITO) and Au electrode surfaces. The polythiophene macro-RAFT agent was electrodeposited by cyclic voltammetry (CV) from thiobenzoate-functionalized terthiophene monomers. The ultrathin films on Au surfaces were investigated using atomic force microscopy (AFM), static contact angle, X-ray photoelectron spectroscopy (XPS), and ellipsometry. On the other hand, the RAFT agent-modified ITO substrate was monitored by UV−vis to track the electropolymerization of the RAFT agent and formation of π-conjugated polymer. Molecular weight (MW) and polydispersity index (PDI) were determined from sacrificial polymerization in solution. AFM imaging revealed typical polymer layer morphology for the films. Investigation of film thicknesses by ellipsometry and AFM profilometry gave comparable results. XPS showed atomic percentages close to expected values, accounting for variations based on component thickness and XPS sensitivity. Diblock copolymer brush formation revealed capabilities of a conventional SI-RAFT procedure using a polythiophene macroinitiator film.

Introduction

Through the years, different techniques have been developed to fabricate polymeric ultrathin films. This includes spin coating,[1] Langmuir−Blodgett techniques,[2] layer-by-layer self-assembly,[3] and surface- initiated polymerization (SIP).[4] The latter method has the advantage of tethering polymers onto the surface with high grafting densities, which is ideal for coating surfaces. Surface modification with surface-initiated grafted polymers prepared via physisorption onto the surface or chemisorption by covalent bonding has been well-documented.[5] Modification of controlled living radical polymerization (CLRP) techniques such as reversible addition−fragmentation chain transfer (RAFT) polymerization to surface-initiated RAFT or SI-RAFT permits the synthesis of tethered polymers with different functionalities exhibiting good control over molecular weight (MW), polydispersity index (PDI), composition, and macromolecular architectures.[6] It provides a powerful tool for tailoring functionality and thickness of nanostructured coatings. The grafting of the initiators is usually done through self-assembled monolayers (SAM)s or adsorbed macroinitiators.

π-Conjugated or electrically conducting polymers have been investigated with respect to their synthesis, properties, and characterization.[7] Their potential applications range from sensors,[8] electro-optical materials,[9] and semiconducting devices.[10] Electropolymerization of heteroaromatic monomers to form π-conjugated polymers or intrinsically conducting polymers (ICP)s has been well-documented.[11] The study of electropolymerizable monomers such as thiophene, aniline, pyrrole, and carbazole is of interest, as it can yield unique polymerization mechanisms and electro-optical applications. It could also lead to interesting electrochromic properties. Polythiophenes in particular is one of the most well-studied polymeric systems.[12] It has been shown in the past that electropolymerization of terthiophene leads to the formation of highly electrochromic and conducting polythiophenes.[13] The mechanism goes through a radical cation coupling which can be accessed through potentiodynamic or potentiostatic methods.[13,14] We have been reporting the deposition of high optical quality ultrathin films of conjugated polymer networks on conducting substrates via electrochemical methods.[15] This "polymer precursor" route, in which electro-active monomers are tethered to a desired polymer backbone or dendrimer, enable the combined macromolecular properties of two polymers. This method is applicable to a variety of systems with different polymer backbones and monomer units, imparting thermal stability/flexibility, improved adhesion, morphological regularity, high optical transparency, and controlled ion permeability. We have reported various routes toward polythiophenes combined with polysiloxanes[16] and polystyrene.[17] The electro-copolymerization between polycarbazole and polythiophene combined with polymethacrylate and their electrochromic properties has been previously studied by our group.[18] To this regard, grafting another polymer adlayer from a conjugated polymer film such as polythiophene can provide another opportunity to combine two polymers as "layered films" which takes advantage of the two polymer materials' properties. Electrodeposition of a conducting polymer macroinitiator on a flat electrode substrate is a plausible route. Electropolymerization is widely utilized for conducting polymer synthesis.[7] The use of the electropolymerization method in immobilizing initiators or CTA on surfaces also has the advantage of employing only one type of electro-active initiator or CTA to any conducting substrates, which avoids the synthesis of different types of surface-coupling agents specific for different functionality of different substrates. To our knowledge, there has been no previous attempt to demonstrate RAFT polymerization

*Corresponding author: Tel 713-743-1760; Fax 7137431756; e-mail radvincula@uh.edu.

 Published on Web 01/19/2011

Scheme 1. General Route for Preparing Homopolymer and Block Copolymers from Electrochemically Deposited Terthiophene CTA

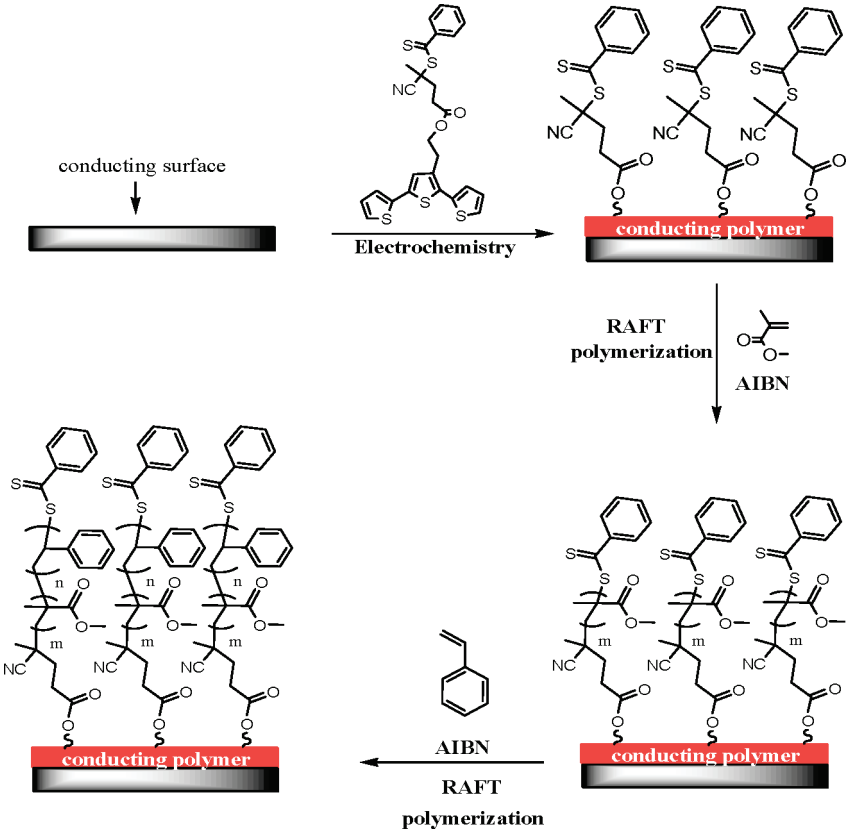

from electrodeposited polythiophenes on a substrate like indium−tin oxide (ITO) or Au glass.[19]

In this study, we have focused on the electropolymerization of a terthiophene monomer bearing a dithiobenzoate moiety, 2-(thiophen-3-yl)ethyl 4-cyano-4-(phenylcarbonothioylthio)pentanoate 2-(2,5-di(thiophen-2-yl)thiophen-3-yl)ethanol, with subsequent deposition as polyterthiophene or polythiophenes on flat electrode surfaces. This led to the attachment of the chain transfer agent (CTA) as macroinitiators on the surface, with the electro-optical properties of polythiophene.[20] These films then underwent SI-RAFT polymerization to obtain surface-anchored polymers (Scheme 1) and were characterized accordingly.[21] Herein we report a new route to forming surface-grafted polymers through the electropolymerization of electro-active CTA moieties followed by the homo- and diblock RAFT polymerization of different monomers from the surface.[22]

Experimental Part

Materials. Chemical reagents were purchased from Aldrich and used without further purification unless otherwise indicated. Tetrahydrofuran (THF) solvent used in the syntheses was distilled from sodium benzophenone. Styrene (Sty) and *tert*-butyl acrylate (TBA) monomers were passed through a column of activated basic alumina to remove the inhibitor. The radical initiator 2,2-azobis(isobutyronitrile) (AIBN) was recrystallized twice from ethanol.

Synthesis of 4-Cyano-4-((thiobenzoyl)sulfanyl)pentanoic Acid[23]. 4,4′-Azobis(4-cyanovaleric acid) (4.19 g, 0.0149 mol) and bis-(thiobenzoyl) disulfide (3.07 g, 0.01 mol) were dissolved in ethyl acetate (200 mL) in a 500 mL round-bottom flask equipped with a condenser. The mixture was degassed by bubbling N_2 and heated to reflux for 20 h under N_2. The reaction was cooled to room temperature, and the solvent was removed under vacuum. The crude product was purified by column chromatography (silica gel) with ethyl acetate:hexanes 2:3 as mobile phase. After solvent removal 4-cyano-4-((thiobenzoyl)sulfanyl)pentanoic acid was obtained as a red oil. The product solidified upon sitting at −20 °C. ^{1}H NMR ($CDCl_3$) δ (ppm): 1.93 (s, 3H, CH_3); 2.38−2.80 (m, 4H, CH_2CH_2); 7.42 (m, 2H, *m*-ArH); 7.56 (t, 1H, J = 8 Hz *p*-ArH); 7.91 (d, 2H, J = 7.3 Hz, *o*-ArH). ^{13}C NMR ($CDCl_3$) δ (ppm): 24.1, 29.5, 32.9, 45.6, 118.4, 126.7, 128.6, 133.1, 144.4, 177.3, 222.1.

Synthesis of Ethyl 2-(2,5-Di(thiophen-2-yl)thiophen-3-yl)acetate (3T-ET) [*Scheme 2*]. Production of 3T-ET was achieved by first synthesizing ethyl 2-(2,5-dibromothiophen-3-yl)acetate as reported in the literature.[18] The procedure was modified to synthesize 3T-ET. Ethyl 2-(2,5-dibromothiophen-3-yl)acetate (6.4 g, 10 mmol) and 2-(tributylstanny1)thiophene (15 g, 20 mmol) were added to a 30 mL dry DMF solution of dichlorobis-(triphenylphosphine)palladium (1.3 g, 1.5 mmol). After three freeze−thaw cycles, the mixture was heated to 100 °C for 48 h. The mixture was cooled to room temperature, poured into a beaker containing 150 mL of water, and extracted with CH_2Cl_2, and the solution was dried with anhydrous Na_2SO_4. After filtration and evaporation of the solvent, the crude product was purified by chromatography on silica gel using toluene as an eluent. The final product was obtained in 85% yield as pale yellow oil. The characterization of the compound was in good agreement with the literature.[18]

Synthesis of 2-(2,5-Di(thiophen-2-yl)thiophen-3-yl)ethanol (3TOH) [*Scheme 2*]. The compound 3T-ET (2 g, 5.9 mmol) in 10 mL of THF was added dropwise, under nitrogen, to an ice-cooled 100 mL THF suspension of (0.32 g, 8.4 mmol) $LiAlH_4$ obtaining a red solution. After complete addition, the ice bath was removed, and the reaction was allowed to warm to room temperature and left stirring for 12 h. The reaction was quenched by adding water and neutralized with a 2 N HCl solution. The red solution immediately turned yellow upon neutralization. The solvent was evaporated, and the resulting mixture was extracted three times using CH_2Cl_2. The combined CH_2Cl_2 extract was again washed with water and brine and dried with Na_2SO_4. After filtration and evaporation the product

Scheme 2. Synthesis of the Electroactive Terthiophene RAFT Agent

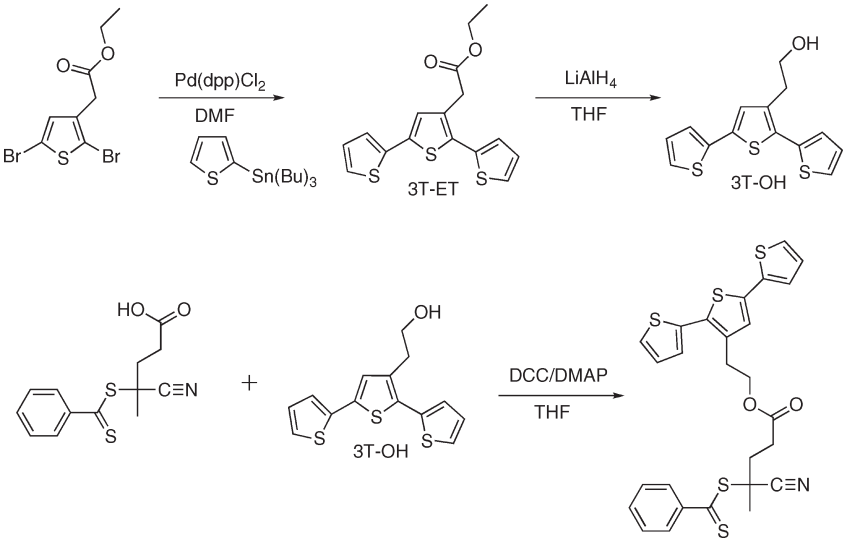

was purified by column chromatography using (4:1) CH_2Cl_2/hexane as an eluent. The final product obtained in 90% yield was oil, which solidified upon vacuum or even at room temperature if kept for a longer time. ^{1}H NMR in $CDCl_3$ δ (ppm): 7.31−7.04 (m, 7H), 3.88 (q, 2H, J = 6.4 Hz), 3.01 (t, 2H, J = 6.4 Hz). ^{13}C NMR: 136.8, 135.8, 135.7, 135.2, 131.2, 127.8, 127.5, 126.4, 126.3, 125.7, 124.6, 123.8, 62.7, 32.4.

Synthesis of 2-(Thiophen-3-yl)ethyl 4-Cyano-4-(phenylcarbonothioylthio)pentanoate 2-(2,5-Di(thiophen-2-yl)thiophen-3-yl)ethanol (CTA). In a 100 mL round-bottom flask equipped with a stir bar and an addition funnel, 10 mL of dry CH_2Cl_2 solution of 4-cyano-4-((thiobenzoyl)sulfanyl)pentanoic acid (0.300 g, 1 mmol), 2-(2,5-di(thiophen-2-yl)thiophen-3-yl)ethanol (0.251 g, 1.1 mmol), and 4-(dimethylamino)pyridine (DMAP) (11.13 mg, 0.091 mmol) was cooled to 0 °C under N_2. Dicyclocarbodiimide (DCC), (0.171 g, 1.1 mmol) was dissolved in 1.40 mL of CH_2Cl_2 and added dropwise to the reaction flask under stirring. After complete addition of DCC, the reaction was stirred for 5 min at 0 °C and then allowed to warm to room temperature overnight. Then, the solid was removed by filtration, and the filtrate was washed with diluted aqueous sodium bicarbonate (20 mL) and water (2 × 20 mL) and finally dried over anhydrous $MgSO_4$. The solution was filtered, and the solvent was removed to yield the crude product as red oil, which was further purified by column chromatography on silica gel using 4:6 hexane/ethyl acetate as eluent. The final product was obtained as a red solid (0.071 g, 12.8% yield). ^{1}H NMR ($CDCl_3$) δ (ppm): 1.88 (s, 3H, $-CH_3$); 2.34−2.67 (m, 4H, CH_2CH_2); 2.94−3.0 (t, 2H, $-CH_2$, J = 6.9); 4.23−4.35 (t, 2H, $-OCHH_2$, J = 6.9); 6.98−7.35 (m, 7H, terthiophene-H); 7.38−7.40 (d, 2H, J = 7.8 *m*-ArH); 7.55 (t, 1H, *p*-ArH, J = 7.2); 7.89−7.86 (dd, *o*-ArH, 2H, J = 9 Hz, J = 1.5). ^{13}C NMR ($CDCl_3$) δ (ppm): 24.0, 28.3, 29.8, 33.2, 45.6, 64.4, 118.4, 123.8, 124.6, 125.8, 126.1, 126.4, 126.6, 127.6, 127.9, 128.5, 131.3, 132.9, 134.6, 135.0, 136.6, 144.5, 171.3, 222.1 Elemental analysis calculated for $C_{27}H_{23}NO_2S_5$: C, 58.56; H, 4.19; N, 2.53; O, 5.78; S, 28.95. Found: C, 58.83; H, 4.36; N, 2.69; O, 5.72; S, 28.65.

Synthesis of 2-(9H-Carbazol-9-yl)ethyl Methacrylate, M1[24]. A solution of methacryloyl chloride (1.55 mL, 15 mmol) in dry THF (10 mL) was added slowly to a solution of triethylamine (1.66 mL, 12 mmol) and 2-(9*H*-carbazol-9-yl)ethanol (2.11 g, 10 mmol) in dry THF (20 mL). The reaction mixture was stirred overnight at room temperature. The ammonium salt was removed by filtration, and the solvent was removed by evaporation. The residue was extracted with dichloromethane, purified by silica-gel column chromatography using petroleum ether/ethyl acetate (5:1) as eluent, and further purified by recrystallization in ethanol (1.58 g, 50% yield). ^{1}H NMR (300 MHz, $CDCl_3$): 8.10 (d, 2H), 7.49 (m, 4H), 7.26 (m, 2H), 5.92 (s, 1H), 5.47 (s, 1H), 4.61 (t, 2H), 4.53 (t, 2H), 1.80 (s, 3H). Elemental analysis calculated for $C_{18}H_{17}NO_2$: C, 77.40; H, 6.13; N, 5.01. Found: C, 77.28; H, 6.24; N, 4.91.

Electrochemical Synthesis of Polymer Film CTA. Film formation of the CTA was studied using the potentiodynamic cyclic voltammetry (CV) technique.[25] In a three-electrode cell, 0.1 M tetrabutylammonium hexafluorophosphate (TBAH) as supporting electrolyte and 5 mM of the CTA in dry THF were mixed and stirred, sweeping the voltage at a scan rate of 50 mV/s 0 to 1.3 V against Ag/AgCl as a reference electrode and platinum as a counter electrode. ITO-glass and Au-glass substrates were used as working electrodes and also as the deposition substrates for growing the polymer brushes.

Synthesis of Grafted Poly(carbazole ethyl methacrylate) (PCzEMA) via RAFT Polymerization (Typical Grafting Procedure). Specified amounts of the CTA (0.002 47 g, 4.48×10^{-6} mol), AIBN (0.000 149 g, 8.96×10^{-7} mol), and carbazole ethyl methacrylate (CzEMA) (0.500 g, 1.79×10^{-3} mol) were added to a 50 mL Schlenk flask. Polymerizations were performed under homogeneous conditions with 5 mL of dry THF as solvent. The monomer mixture was degassed by bubbling pure nitrogen for 1 h and transferred to a second Schlenk tube containing the CTA-modified Au substrate backfilled with nitrogen via cannula process. The septum-sealed flask was then placed in an oil bath at 60 °C. After 18 h, the slide was removed and the free polymers were quenched to 0 °C. Untethered polymer was removed from the substrate via Soxhlet extraction overnight at 60 °C in THF. Free polymer from the polymerization solution was precipitated from MeOH. This procedure was repeated until no monomer signals were observed in ^{1}H NMR. The resulting polymer material was then dried under vacuum at room temperature until no weight loss was observed and then analyzed by gel permeation chromatography (GPC). The polymer film was also dried under vacuum for 24 h and was subsequently characterized using a variety of surface analytical methods.

Characterization. NMR spectra were recorded on a General Electric QE-300 spectrometer at 300 MHz. UV−vis spectra were recorded on an Agilent 8453 spectrometer. GPC was carried out on a Viscotek 270 instrument with a triple detector array (RALS, IV, RI, or UV) equipped with 2 GMHHR-M and 1 GMHHR-L mixed bed ViscoGel columns (eluent: THF; flow rate: 1 mL min^{-1}). CV was performed on a Parstat 2263 (Princeton Applied Research) instrument using PowerSuite software. All experiments were carried out using a three-electrode

setup using platinum wire as the counter electrode, Ag/AgCl as the reference electrode, and either ITO or gold as working electrodes, pretreated according to the literature.[26] Atomic force microscopy (AFM) imaging was performed under ambient conditions with a PicoScan 2500 (Agilent Technologies formerly Molecular Imaging, Corp.) in the intermittent contact mode. Ellipsometric measurements were carried out using the Multiskop, Optrel GbR with a 632.8 nm helium−neon laser at 60° angle of incidence. Refractive indices were fixed at 1.50 for all respective surface modifications except for polystyrene (PSty) and polymethylmethacrylate (PMMA), which were 1.55 and 1.49, respectively. The Au-glass electrodes were cleaned with a plasma ion cleaner (Plasmod, March). X-ray photoelectron spectroscopy (XPS) was carried out in a Physical Electronics 5700 instrument with photoelectrons generated by the nonmonochromatic Al Kα irradiation (1486.6 eV). Photoelectrons were collected at a takeoff angle of 45° using a hemispherical analyzer operated in the fixed retard ratio mode with an energy resolution setting of 11.75 eV. The binding energy scale was calibrated prior to analysis using the Cu $2p_{3/2}$ and Ag $3d_{5/2}$ lines. Charge neutralization was ensured through cobombardment of the irradiated area with an electron beam and the use of the nonmonochromated Al Kα source. This placed the adventitious C 1s peak at a binding energy of 284.6 ± 0.2 eV.

Results and Discussion

CLRP techniques adapted to surface-initiated polymerization (SIP) have received much attention due to their ability to mediate controlled grafting of polymers on surfaces with many advantages including controlled thickness, film homogeneity, morphological uniformity, and the possibility for synthesis of complex macromolecular architectures.[26,27] RAFT polymerization offers many advantages to synthesize a variety of polymer architectures with many types of monomers including hydrophilic monomers.[28] The direct immobilization of a CTA is the best method to tether polymer chains on surfaces by RAFT. There are a several examples in the literature where the immobilization of the CTAs enabled the "grafting from" technique to be implemented.[21,22] The CTAs are primarily immobilized by modification of the surfaces by Grignard reagents, condensation reactions, and SAMs of alkylthiol and alkoxysilane containing RAFT CTAs. Others have reported the modification of the surface with an ATRP agent that subsequently was modified with a RAFT agent.[21,29] In this work we have focused on the grafting of homopolymer and diblock copolymer chains through immobilized macro-RAFT CTAs by electropolymerization. A consequence of this is that an electro-optically active or conducting polymer film such as polythiophene is also grafted underneath the grafted polymer layer.

Electrodeposition of a RAFT CTA Agent on Au and ITO Surfaces [Scheme 1]. The Au-glass or ITO-glass substrate was initially cleaned using a plasma ion cleaner (Plasmod, March). The electropolymerization was then performed in a three-electrode cell, with a solution of the terthiophene−CTA molecule in THF (5 mM) and 0.1 M TBAH. This was done potentiodynamically at 50 mV/s by sweeping the potential from 0 to 1300 mV versus the Ag/AgCl reference electrode and Pt counter electrode. As the onset of oxidation begins on the first cycle, an increase in current after 1.1 V is observed due to polymer deposition (Figure 1). On the cathodic sweep, there is a negative current due to removal of the supporting anion from the polymer, i.e., reduction of the polyterthiophene from the conducting to insulating form. Continuous cycling up to 10 cycles does not change the CV shape and the current increases with each cycle, but the onset of oxidation is eventually lowered to 0.5 V. With the particular conditions used, over time, this led to the formation of a polymer film that could be reversibly cycled between the neutral polymer, red in color, and the oxidized form, which was black. The substrate was then taken out and rinsed with THF, acetone, and CH_2Cl_2 and dried under vacuum/N_2. The surface modification with the macro-RAFT CTA was confirmed by ellipsometry, static water contact angle, AFM, and XPS. The electrodeposited film at 10 cycles gave an average thickness of 2.43 ± 0.83 nm. The contact angle measured gave an average value of 85.7 ± 1.6°. The standard deviation and the ultimate thickness limit can be influenced by the fact that electropolymerization depends on a number of parameters including scan rate, solvent, concentration, and type of supporting electrolyte (see Supporting Information). The results for the different conditions are summarized in Table 1. In principle, nucleation on the surface with electropolymerization will eventually induce the formation of oligomers and then polymers, which precipitate out. This precipitation process can account for thickness variations, underscoring the need for optimized electropolymerization conditions. What is clear from Table 1 is that this electrodeposition though well-behaved forms relatively thin films (Table 2) as evidenced by the low currents, with electrochemical properties nearly the same for a variety of conditions. Dissolved polymers were also observed in solution with an increase in deep red color of the solution over time (Supporting Information). Nevertheless, XPS measurements confirmed the modification of the Au surface with the macro-RAFT CTA (discussed later). In the past, the problem of increasing the overall oxidation potential due to introduction of substituents has been overcome by extending the conjugation length of the monomer to a dimer and trimer, resulting in a significant reduction of the overall oxidation potential.[30] The anodic peak at ca. 0.86 V, corresponding to the oxidation of polymeric terthiophene was observed for the ITO substrate scan (Figure 1). The oxidation onset becomes lower at 0.6 V in the second cycle onward.[31] This behavior is typical for polythiophenes in which the higher conjugated polymer species formed resulted in a lower oxidation potential onset for doping. It is possible to observe one- or two-electron-transfer processes depending on the conditions of electropolymerization.[32]

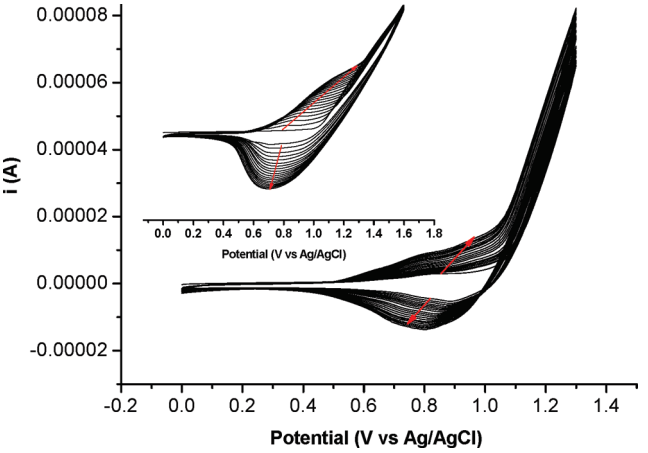

Figure 1. Cyclic voltammogram (CV) of 1.5 mM terthiophene monomer solution in THF with 0.1 M TBAH on ITO. The polymerization was performed by sweeping the potential from 0 to 1300 mV vs Ag/AgCl reference electrode. Shown inset is the copolymerization with carbazole monomer 50:50 on gold (the same conditions).

The peak potential shifted to higher values as the thickness of the film increased. This potential shift is attributed to heterogeneous electron-transfer kinetics, *IR* drop of the film ($V_{total} = V_{across\ film} + I[R_{film} + R_{soln}]$), and a decrease of the film conductivity.[33] The corresponding reduction peak was

Table 1. Peak Anodic and Cathodic Currents/Potentials and Their Corresponding Onset of Oxidation Potential (First Cycle)[a]

parameters	onset	E_{pa} (V)	i_{pa} (mA)	E_{pc} (V)	i_{pc} (mA)
50 mV/s, 10 cycles, 1.5 mM, ITO	1.1	0.86	0.02	0.76	−0.02
50 mV/s, 10 cycles, 6.0 mM, ITO	0.91	0.81	0.02	0.86	−0.02
50 mV/s, 10 cycles, 1.5 mM, Au	1.1	0.79	0.02	0.82	−0.02
50 mV/s, 20 cycles, 0.75 mM, Au with 50:50, terthiophene:carbazole	1.1	0.9	0.04	0.82	−0.04
50 mV/s, 20 cycles, 1.5 mM, Au with 50:50, terthiophene:carbazole	1.1	0.9	0.08	0.71	−0.07

[a] Peak anodic potential, E_{pa} (V); peak anodic current, i_{pa} (mA); peak cathodic potential, E_{pc} (V), peak cathodic current, i_{pc} (mA).

Table 2. Thickness and Contact Angle Data for Homopolymer and Diblock Copolymer Films

		water contact angle (deg)[b]	
structure	Δ thickness (nm)[a]	θ left	θ right
electrografted CTA	2.4	85.71	82.03
PMMA	25.5	67.79	69.19
PMMA-*b*-PSty	32.1	85.55	86.43
PMMA-*b*-PStyPF	31.9	98.31	97.64
PCzEMA	28.4	67.36	66.98
PTBA	35.4	64.3	63.1
PSty	7.2	68.92	67.74

[a] Thicknesses were determined by ellipsometry and are an average of five samplings across the sample. Error of thicknesses measured was within ±1 nm. The thickness measured is additive from the last layer measured, i.e., PMMA thickness. [b] Water contact angles measurements were taken across the sample and are an average of five measurements. The standard deviation is less than 3°.

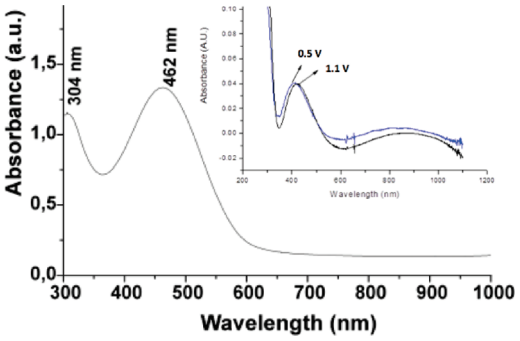

Figure 2. UV−vis spectrum of the electrodeposited CTA film on ITO-glass coated substrate, electropolymerized at 50 mV/s scan rate and sweep potential from 0 to 1 300 mV in THF. Shown inset is the spectroelectrochemical scan of the same film at 0.5 and 1.1. V showing the formation of a band from 600 to 1000 nm, indicating polaronic and bipolaronic species of the doped polythiophene.

observed at around 0.86 V which is attributed to the dedoping of the polythiophene. Interestingly, we also attempted to coelectropolymerize the CTA with carbazole monomer at 50:50 ratio with different concentrations under the same conditions above (Figure 1 inset). Thicker films were observed with higher current densities per cycle. The CV is also well-behaved. Recently, the use of carbazole to copolymerize with thiophene and terthiophene monomers has been shown as a way of improving the electrodeposition behavior of conducting polymers.[17,18] While these films were not used for SI-RAFT per se, this demonstrates that several parameters including coelectropolymerization with another monomer should enable variations on the electro-optical properties or even perhaps the density of the CTA species on the macroinitiator film.

Spectroscopic Properties. The UV−vis spectrum of the electropolymerized CTA film on-ITO coated glass was (Figure 2) obtained from the film deposited on an ITO-glass substrate at 0.0 V. The absorption spectra is characterized by two broad peaks at 304 and 462 nm, attributed to the $\pi-\pi^*$ transition of the thiobenzoate and polythiophene peak absorption, respectively.[34] The presence of the peak at 304 nm is important as this represents preservation of the thiobenzoate moiety for subsequent surface-initiated polymerization. This peak is not observed in electropolymerized unmodified terthiophene monomers.[36]

With spectroelectrochemistry, an increase of potential to 0.5 and 1.0 V results in a decrease in the peak at 464 nm as well as appearance of a band toward the near-IR region ~600−1000 nm (Figure 2, inset).[36] It is well accepted that this peak shift arise due to transitions from the valence band to the conduction band and polaron bonding level or π^* conduction band of polythiophene respectively upon doping.[12] Caspar et al. specifically attributed the bands in this region to terthiophene bipolarons, suggesting that the quinoid resonance structure of the bipolaron would be stable and would be analogous to the site of charged storage in bulk polythiophene.[35] Because of the relatively poor adhesion once the polymer is formed, some of the isolated formed polymers were also observed in solution. The oxidized or doped state of this polymer is evident with a peak at 472 and 880 nm (Supporting Information). Thus, these films are considered to be typical of electrodeposited polyterthiophene films.[35,36]

Surface-Initiated Polymerization. In order to probe the effectiveness of the macro-CTA modified Au-glass substrate to grow polymer chains from the surface, four different monomers were polymerized including styrene (Sty), pentafluorostyrene (StyPF) methyl methacrylate (MMA), *tert*-butyl acrylate (TBA), and carbazole ethyl methacrylate (CzEMA) by SI-RAFT polymerization (Scheme 3). For brevity, we describe only the typical procedure using the CzEMA monomer. The procedure for the rest of the monomers is similar. The molar ratio between monomer, initiator and CTA were 400:0.2:1 (for CzEMA); the reaction was performed for 8 h at 60 °C. Free CTA in solution and free polymer were isolated and analyzed in order to estimate the M_n and PDI of the grafted polymer on the surface. For PCzEMA, a number-average molecular weight, M_n = 67 719 g mol^{-1}, and PDI = 1.15 were obtained, showing good control over the polymerization reaction conditions. Other characterization data of this polymer product such as NMR and thermogravimetric analysis (TGA) are shown in the Supporting Information. The obtained films were washed initially with THF and toluene and subsequently underwent Sohxlet extraction prior to characterization. Ellipsometric measurements of this particular film showed an increase in thickness from 2.4 nm (electrodeposited macroinitiator) to 28.4 nm, after RAFT polymerization of the CzEMA. This demonstrated the ability of the macroinitiator modified gold surface to initiate polymerization. Contact angle measurements showed a decrease from 85° to 67° after RAFT homopolymer grafting, indicating an increase in hydrophilicity of the surface. A summary of the ellipsometric thickness results and contact angle−wetting behavior of the different polymers grafted is shown in Table 2.

The MWs and the PDIs for the other polymers were determined similarly from the sacrificial polymerization in solution (Table 3). Copolymerization of PMMA with

Scheme 3. Synthetic Scheme for the Fabrication of Homopolymer and Block Copolymer Brushes from Electrodeposited Polythiophene CTA

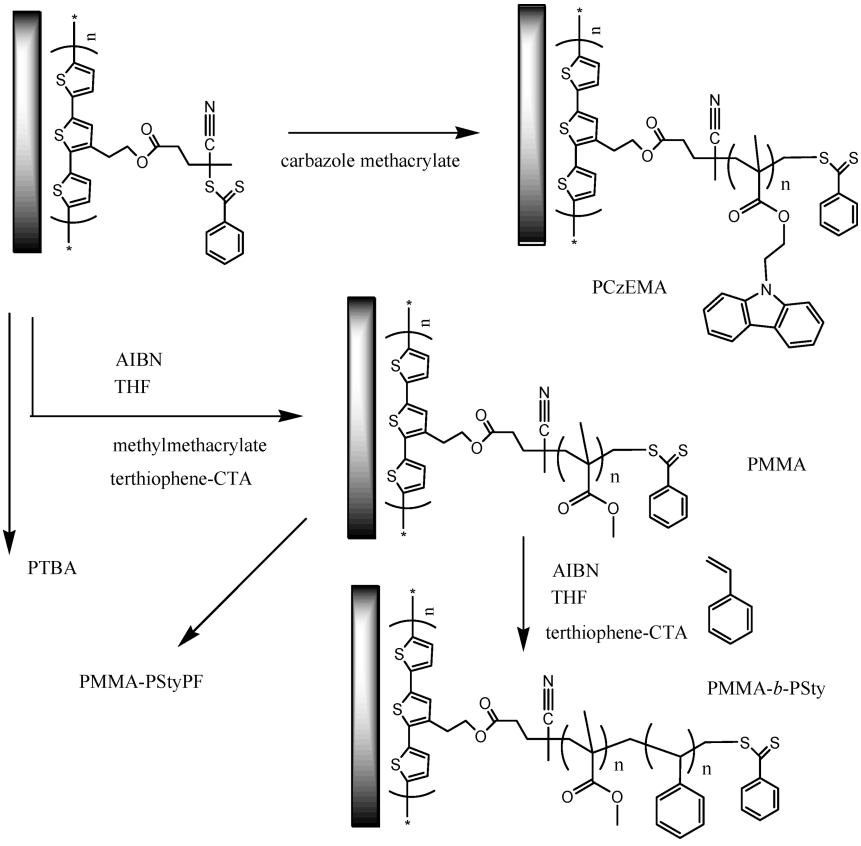

Table 3. Molecular Weights and Properties of Solution Polymerizations Determined by Gel Permeation Chromatography

polymer	theoretical M_n (g mol^{-1})	experimental M_n (g mol^{-1})	PDI
PMMA[a]	35 548	37 835	1.14
PMMA-*b*-PSty[b]	N.D.	57 625	1.25
PCzEMA[c]	67 928	67 519	1.15
PMMA-*b*-PStyPF[d]	N.D.	48 920	1.35
PTBA[e]	41 568	45 589	1.24

[a] PMMA synthesized using a monomer:CTA ratio of 500:1 and CTA:initiator (AIBN) 5:1, 24 h of reaction, in THF at 60 °C. [b] Synthesized using a molar ratio between monomer:macro-CTA 500:1, CTA:initiator(AIBN) 5:1, 24 h of reaction, THF as solvent at 60 °C. [c] Monomer:CTA ratio of 400:1 and CTA:initiator (AIBN) 5:1, 18 h of reaction, in THF at 60 °C. [d] Macro-monomer:CTA 500:1 and CTA:initiator (AIBN) 5:1, 22 h of reaction, in THF at 60 °C. [e] Monomer:CTA ratio of 500:1 and CTA:initiator (AIBN) 5:1, 24 h of reaction, in THF at 60 °C.

more hydrophobic monomers (styrene and pentafluorinated styrene) was done in order to assess the ability to form more complex macromolecular architectures. The PMMA-grafted film was first prepared by SI-RAFT polymerization, i.e., using similar conditions to the synthesis of the PCzEMA-grafted chains. The grafting polymerization of the styrene and pentafluorinated styrene resulted in thicker films and more hydrophobic character as characterized by contact angle measurements (Table 2). The increase in thickness over the previous PMMA block is obvious. Since any physically adsorbed polymers have been removed by Sohxlet extraction, the remaining thickness increase can only be attributed to the grafted second block.

At this point, it is important to discuss the difference between RAFT polymerization with the Z or R group approach. In accordance with convention for our CTA, the R group is the tertiary carbon with the nitrile group and the Z group is the phenyl ring (Scheme 2). Several groups have done SI-RAFT via the Z group approach.[37] In their case, the RAFT agent is covalently attached to the surface via the Z group, which closely resembles a "grafting to" approach in mechanism, i.e., becomes more diffusion controlled as the MW is increased and has a propensity to form films with low grafting densities. The most promising means of forming high density and uniform grafted polymer chains is via attachment of the CTA through the R group as demonstrated by Boyes et al.[21] This method is truly a "grafting from" technique which relies mainly on monomer diffusion and equilibration with sacrificial initiators. Several approaches have been taken to tether polymers through R group attachment of the CTAs.[38] Our approach in this case is similar to Boyes et al. except that the initiator-CTA is already formed whereas in their approach, it is generated in situ.[21] The thickness/MW correlation were found to be consistent with their results, e.g., M_n = 37 835 g/mol with a thickness of 23.1 nm in our case and M_n = 21 910 g/mol with thickness of 15.2 nm in theirs.

Morphology Studies. The film growth and change in morphology were also investigated by AFM using the intermittent contact mode ac or MAC mode (Figure 3). Note that all these images were unannealed morphologies—as solvent washed or with Soxhlet extraction procedure. Figure 3a shows the morphology of the polymer obtained after electrochemical deposition of the CTA on Au-glass. A homogeneous

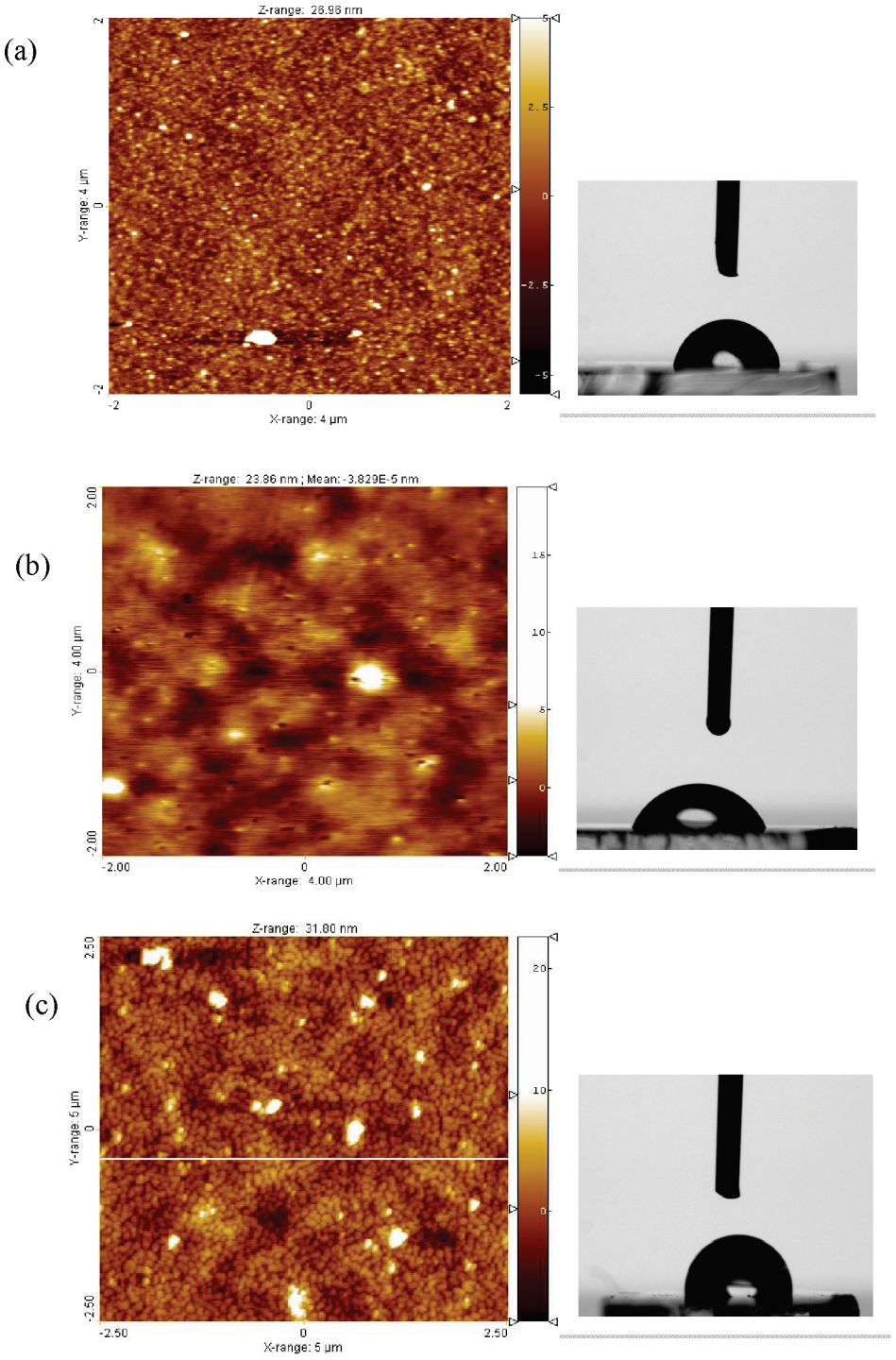

Figure 3. AFM images and contact angle of the gold modified-CTA: (a) after CTA electropolymerization, (b) after PMMA brush synthesis, (c) after PMMA-*b*-PSTy diblock copolymer brush synthesis. Shown inset is the corresponding water contact angle. Original Au-glass surface is shown in the Supporting Information.

and morphologically continuous film was formed on the substrate with very small domain sizes that are different from Au-glass (Supporting Information). The average height is 2.9 nm (rms roughness = 1.5 nm) as measured by AFM profilometry (consistent with ellipsometry) and associated with a normal contact angle showing a hydrophobic surface (83°). After PMMA brush formation (Figure 3b), the films are less smooth and more undulating with larger domain regions, although some aggregation can be noticed. A thickness of 25 nm was obtained by profilometry with the (rms roughness = 1.7 nm), in agreement again with ellipsometry measurements, which indicated an increase of 22 nm over the 2.8 nm thick CTA film. Contact angle showed that the surface has a lower hydrophobic character (68°).

Figure 3c shows the morphology of the diblock copolymer (PMMA-*b*-PSty) after several washings and Soxhlet extraction procedures with THF, acetonitrile, and dichloromethane. It is observed to form more granular aggregates (average height: 31.80 with 2.6 nm rms roughness), with an increase in thickness of ~7 nm attributed to the grafted PSty block—again consistent with ellipsometric measurement after the diblock copolymer synthesis. This film also showed

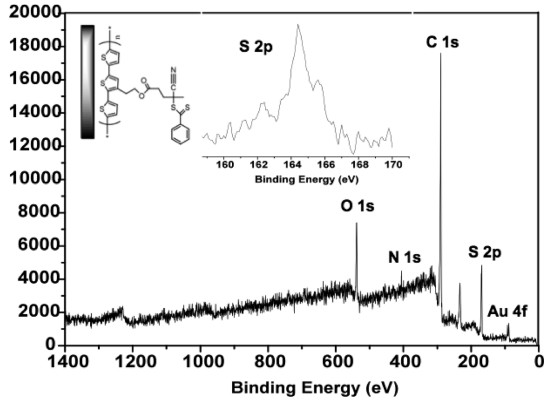

Figure 4. Wide-scan X-ray photoelectron spectra of the electrodeposited macro-CTA agent and the high-resolution S 2p scan (inset).

Table 4. Actual Atomic Percentage of Polymer-Modified Gold Substrates from Wide-Scan X-ray Photoelectron Spectroscopy[a]

surface structure	C 1s	O 1s	N 1s	S 2p	F 1s
electrografted CTA	57.6	10.8	2.8	10.2	N.A.
PMMA	72.3	24.6	< 0.1	0.3	N.A.
PMMA-*b*-PSty	83.3	15.3	0.8	0.25	N.A.
PMMA-*b*-PStyPf	60.9	9.9	< 0.1	< 0.1	27.8
PTBA	62.4	29.4	5.3	1.5	N.A.
PCzEMA	77.4	11.3	11.0	0.2	N.A.

[a] Theoretical atomic percentage of the components of the polymer-modified gold substrates based on monomer repeat unit at nearest whole number multiple: electrografted CTA ($C_{27}H_{23}NO_2S_5$), PMMA ($C_5H_8O_2$), PSty, PTBA($C_7H_{12}O_2$), PStyPF($C_8H_3F_5$), PCzEMA-($C_{18}H_{17}NO_2$). See Supporting Information table.

homogeneity but with a rougher surface compared to PMMA. This roughness is in the form of smaller domains with less undulation. There are more aggregate features compared to PMMA. The normal contact angle showed an increase in the hydrophobic character of the surface (95°) consistent with other PSty films. The morphology of the grafted PCzEMA film is shown in the Supporting Information.

XPS Studies. A successful RAFT mechanism requires that all polymer chains be initiated at the same time from the immobilized CTA. The process has to be monitored for each step up to the formation of tethered diblock copolymers. To characterize the immobilization of the RAFT agent and the growth of the polymer chains, XPS was used to follow the composition (atomic percentages) changes step-by-step. Figure 4 shows the survey scan of the electrodeposited macro-RAFT CTA and the respective binding energies (BE). The high-resolution scan for S 2p is also included. A summary of peak assignments and the actual composition ratios are shown in Table 4. The theoretical values are given in the Supporting Information. The polythiophene composition is in general agreement with the theoretical value calculated for $C_{27}H_{23}NO_2S_5$, except for the C/O ratio (Supporting Information). Also, the Au species is clearly observed at BE 88 and 84 eV because the electrodeposited CTA is only 2.4 nm thick and the penetration depth of a typical XPS methodology is 5−10 nm. The C 1s peak contains the BE of C=C−C at 284.3 eV and C=C−S at 286 eV for thiophene. The appearance of a peak at ~164 eV in the S 2p narrow scan can be attributed both on the S on the thiophene[39] and dithio moiety.[40] In principle, the active dithio moiety of the CTA must not be affected during the electrodeposition process to ensure successful SI-RAFT polymerization. The absence of a peak at ~168 eV suggests the absence of oxidized S on the surface.[41] The presence of the small peak at ~162 eV could

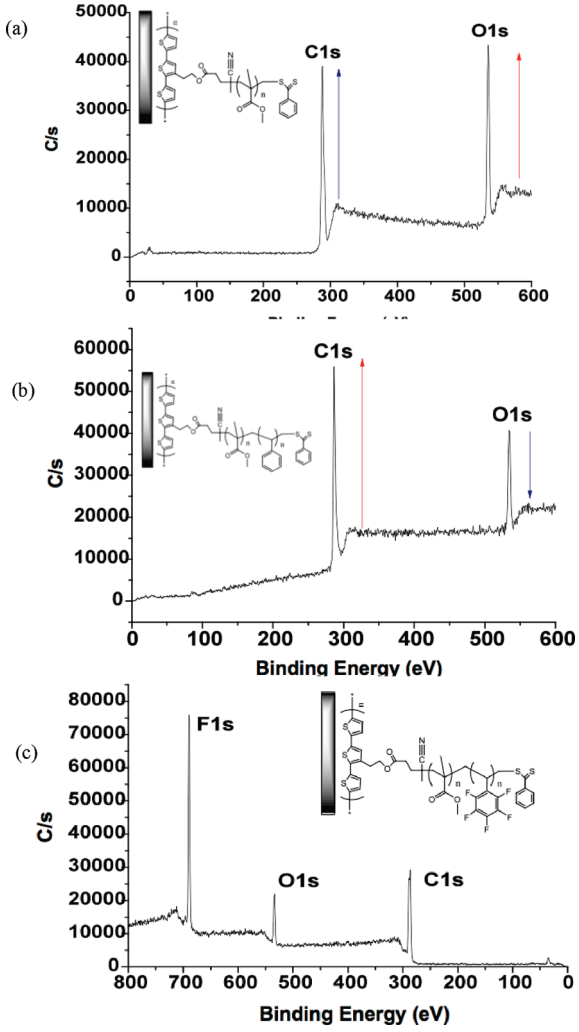

Figure 5. Wide-scan X-ray photoelectron spectra of the (a) PMMA brush homopolymer, (b) PMMA-*b*-PSty diblock copolymer brush, and (c) PMMA-*b*-PStyPF. *Y*-axis is photon counts, and *X*-axis is the binding energy (eV).

represent the chemisorbed S on Au.[42] This peak is expected because of the proximity of the electrodeposited terthiophene moieties on the Au substrate. The main issue will be the possible adsorption of the dithio moiety on the Au surface, which may hinder the activity of the dithio group during the polymerization. If this were the case, polymer growth would not be achieved after the polymerization process. However, upon subjecting the electrodeposited macro-CTA to SI-RAFT polymerization, polymer growth was observed based on thickness measurements, contact angle changes, and XPS measurements, signifying that the dithio group is accessible for mediating the SI-RAFT process. Furthermore, our parallel study on carbazole-based CTA (does not contain thiophene and therefore S on terthiophene moiety is discounted) confirmed that the S is not adsorbed on the Au substrate due to the possible reason that the rate of the electrodeposition process is faster than the rate of adsorption of the dithio moiety on Au.[43]

Figure 5 shows the survey scan for the different grafted polymers, PMMA, PMMA-*b*-PSty diblock, and PMMA-*b*-PStyPF. The XPS spectra of PCzEMA polymer film and the high-resolution spectra for determining the individual atomic species are also given in the Supporting Information, together with the theoretical value for the monomer component with several assumptions. Starting from the electrodeposited

macro-RAFT agent (Figure 4), the values were confirmed by the atomic percentages obtained compared to the theoretical value (Table 4). After PMMA growth by RAFT polymerization, the atomic percentage of C 1s increases from 57.6 to 72.3 and the O 1s band from 7.8 to 24.6, indicating the presence of the PMMA composition (theoretical C/O = 2.9 vs actual C/O = 2.9). This very good agreement benefited from the thick PMMA composition (25.5 nm). On the other hand, the Au 4f disappeared and the N 1s and S 2p decreased from 4.4 and 4.3 to less than 0.5 for both because these elements are only associated with the CTA. The presence of the S 2p in trace amount is important since it also represents the end-group of the PMMA that is capable of further polymerization. The PSty was then grafted on the PMMA brush. From Table 3 and Figure 5, the obvious increase of the C 1s band from 72.3 to 83.3 and the decrease of the O 1s band from 24.6 to 15.3 after PMMA-*b*-PSty synthesis can be observed. Since PSty is only made up of C, the presence of the O 1s indicates that the PSty is relatively thin (6.6 nm) as the spectrum incorporates part of the PMMA brush (31.9 nm, Table 2). The results from the other surface-grafted polymers are also summarized in Table 4. The C 1s and O 1s for the PMMA, PTBA, and N 1s for PCzEMA homopolymer chains are changed as shown in Table 4. For the PMMA-*b*-PStyPF copolymer (Figure 5), the presence of the F 1s due to the Fluorine content of the PStyPf block is observed. The theoretical C/F = 1.6 vs actual C/F = 2.2 indicates that the composition of the PMMA is still detected by the XPS (O is also still present). The PStyPF is again thinner (6.3 nm) compared to the PMMA block. Thus, in each case of polymer brush formation, the presence of free AIBN, monomer, and the electrodeposited CTA ensured a controlled polymerization that corresponded well to the composition/thickness observed on the surface.

Conclusion

We have demonstrated a method for grafting polymers on electrode surfaces by SI-RAFT from an electropolymerized polythiophene macroinitiator film. The synthesis of an electroactive terthiophene R-group CTA was described and subsequently electropolymerized. The electro-optical properties of the deposited polythiophene were confirmed by CV and UV−vis spectroelectrochemistry. These films were then used to obtain PCzEMA, PMMA, PTBA homopolymer brushes, and PMMA-*b*-PSty and PMMA-*b*-PFPSty diblock copolymers by SI-RAFT. Addition of free CTA and AIBN was performed in each case in order to control molecular weight growth from the surface and maintain active "living" end groups. The free polymer chains obtained from the solution were used to estimate the MW and PDI confirming controlled behavior for these reactions. Several characterization techniques including ellipsometry, contact angle measurements, AFM, and XPS confirmed the electropolymerization and electrodeposition of the RAFT agent and subsequent polymerization. In the future, it should be possible to explore various combinations of electroactive polymers and polymer compositions including site directed electropatterning. Kinetic studies of this newly presented method are also underway to further investigate and establish the "polymer brush" behavior under different conditions.

Acknowledgment. The authors acknowledge funding from NSF DMR-10-06776, ARRA-CBET-0854979, CHE-1041300, Texas NHARP 01846, and Robert A. Welch Foundation, E-1551. Technical support from Malvern-Viscotek Inc., Biolin Scientific-KSV Instruments, Agilent Technologies, is also appreciated. C. D. Grande (Universidad del Valle) acknowledges Instituto Colombiano de Investigaciones Científicas, COLCIENCIAS and CENM, Centro de Excelencia en Nuevos Materiales for support. Discussions with Dr. Fabio Zuluaga, Universidad del Valle, Cali, Colombia is also acknowledged.

Supporting Information Available: Electropolymerization data of macro-CTA, AFM images, and XPS spectra of polymer brushes; UV−vis spectra from solution. This material is available free of charge via the Internet http://pubs.acs.org.

References and Notes

(1) Levinson, W.; Arnold, A.; Dehodgins, O. *Polym. Eng. Sci.* **1993**, *33*, 980.
(2) Roberts, G. *Langmuir Blodgett Films*; Plenum Press: New York, 1990.
(3) Decher, G. *Science* **1997**, *277*, 1232.
(4) Advincula, R.; Brittain, W.; Caster, K.; Ruhe, J. *Polymer Brushes: Synthesis, Characterization, Applications*; Wiley-VCH: New York, 2004.
(5) (a) Prucker, O.; Ruhe, J. *Langmuir* **1998**, *14*, 6893. (b) de Soler-Illia, G.; Sanchez, C.; Lebeau, B.; Patarin, J. *Chem. Rev.* **2002**, *102*, 4093–4138. (c) Zhao, Y.; Perrier, S. *Macromolecules* **2006**, *39*, 8603–8608. (d) Advincula, R. *J. Dispersion Sci. Technol.* **2003**, *24*, 343–361. (e) Advincula, R. *Adv. Polym. Sci.* **2006**, *197*, 107–136.
(6) (a) Moad, G.; Rizzardo, E.; Thang, S. *Aust. J. Chem.* **2005**, *58*, 379–410. (b) Perrier, S.; Takolpuckdee, P. *J. Polym. Sci., Part A: Polym. Chem.* **2005**, *43*, 5347–5393. (c) Favier, A.; Charreyre, M. *Macromol. Rapid Commun.* **2006**, *27*, 653–692.
(7) (a) Li, Y.; Vamvounis, G.; Holdcroft, S. *Macromolecules* **2002**, *35*, 6900–6906. (b) Friend, R.; Gymer, R.; Holmes, A.; Burroughes, J.; Marks, R.; Taliani, C.; Bradley, D.; Dos Santos, D.; Bredas, J.; Logdlund, M.; Salaneck, W. *Nature* **1999**, *397*, 121–127. (c) Skotheim, T.; Reynolds, R. *Handbook of Conducting Polymers*; CRC Press: Boca Raton, FL, 2007; 1024 pages.
(8) Wang, X.; Kim, Y.; Drew, C.; Ku, B.; Kumar, J.; Samuelson, L. *Nano Lett.* **2004**, *4* (2), 331–334.
(9) Tong, H.; Wang, L.; Jing, X.; Wang, F. *Macromolecules* **2003**, *36* (8), 2584–2586.
(10) McCullough, R.; Ewbank, P.; Loewe, R. *J. Am. Chem. Soc.* **1997**, *119*, 633–634.
(11) Gaupp, C.; Reynolds, J. *Macromolecules* **2003**, *36*, 6305–6315.
(12) (a) Perepichka, I.; Perepichka, D.; Meng, H.; Wudl, F. *Adv. Mater.* **2005**, *17*, 2281. (b) Perepichka, I.; Perepichka, D. *Handbook of Thiophene Based Materials: Applications in Organic Electronics and Photonics*; Wiley Publishers: New York, 2009; 910 pages.
(13) (a) Evans-Kennedy, U.; Clohessy, J.; Cunnane, V. J. *Macromolecules* **2004**, *37*, 3630–3634. (b) Zotti, G.; Marin, R.; Gallazzi, M. *Chem. Mater.* **1997**, *9*, 2945–2950.
(14) Yassar, A.; Moustrou, C.; Youssoufi, H.; Samat, A.; Guglielmetti, R.; Garnier, F. *Macromolecules* **1995**, *28*, 4548–4553.
(15) (a) Xia, C.; Advincula, R. *Chem. Mater.* **2001**, *13*, 1682. (b) Baba, A.; Onishi, K.; Knoll, W.; Advincula, R. *J. Phys. Chem. B* **2004**, *108*, 18949. (c) Taranekar, P.; Fulghum, T.; Baba, A.; Patton, D.; Ponnapati, R.; Clyde, G.; Advincula, R. *J. Am. Chem. Soc.* **2007**, *129*, 12537. (d) Taranekar, P.; Fan, X.; Advincula, R. *Langmuir* **2002**, *18*, 7943–7952. (e) Fulghum, T.; Karim, S. M. A.; Baba, A.; Taranekar, P.; Nakai, T.; Masuda, T.; Advincula, R. C. *Macromolecules* **2006**, *39*, 1467. (f) Waenkaew, P.; Taranekar, P.; Phanichphant, P.; Advincula, R. *Macrom. Rapid Commun.* **2007**, *28*, 1522. (g) Huang, C.; Jiang, G.; Advincula, R. *Macromolecules* **2008**, *41*, 4661. (h) Jegadesan, S.; Sindhu, S.; Advincula, R.; Valiyaveettil, S. *Langmuir* **2006**, *22*, 3807. (i) Deng, S.; Advincula, R. *Chem. Mater.* **2002**, *14*, 4073. (j) Park, J.; Ponnapati, R.; Taranekar, P.; Advincula, R. *Langmuir* **2010**, *26* (9), 6167. (k) Kaewtong, C.; Jiang, G.; Felipe, J.; Pulpoka, B.; Advincula, R. *ACS Nano* **2008**, *2*, 1533–1542.
(16) Xia, C.; Fan, X.; Park, M.; Advincula, R. *Langmuir* **2001**, *17*, 7893–7898.
(17) Taranekar, P.; Baba, A.; Fulghum, T.; Advincula, R. *Macromolecules* **2005**, *38*, 3679–3687.
(18) Taranekar, P.; Fulghum, T.; Baba, A.; Patton, D.; Advincula, R. *Langmuir* **2007**, *23*, 908.
(19) Liu, J.; Yang, W.; Zareie, H.; Gooding, J.; Davis, T. *Macromolecules* **2009**, *42*, 2931.
(20) Sankaran, B.; Reynolds, R. *Macromolecules* **1997**, *30*, 2582.
(21) Rowe-Konopacki, M.; Boyes, S. *Macromolecules* **2007**, *40*, 879–888.
(22) (a) Boyes, A.; Granville, A.; Baum, M.; Akgun, B.; Mirous, B.; Brittain, W. *Surf. Sci.* **2004**, *570*, 1–12. (b) Roy, D.; Guthrie, J.; Perrier, S. *Macromolecules* **2005**, *38*, 10363–10372.

(23) Thang, S.; Chong, Y.; Mayadunne, T.; Moad, G.; Rizzardo, E. *Tetrahedron Lett*. **1999**, *40*, 2435.
(24) Du, F.; Li, Z.; Hong, W.; Gao, Q.; Li, F. *J. Polym. Sci., Part A: Polym. Chem*. **2000**, *38*, 679.
(25) (a) Ambrose, J.; Carpenter, L.; Nelson, R. *J. Electrochem. Soc*. **1975**, *122*, 876–880. (b) Mengoli, G.; Musiani, M.; Schreck, B.; Zecchin, S. *J. Electroanal. Chem*. **1988**, *246*, 73–86.
(26) (a) Zhao, B.; Brittain, W. *Prog. Polym. Sci*. **2000**, *25*, 677–710. (b) Senaratne, W.; Andruzzi, L.; Ober, C. *Biomacromolecules* **2005**, *6*, 2427–2448.
(27) Matyjaszewski, K.; Davis, T. *Handbook of Radical Polymerization*; Wiley-Interscience: New York, 2002.
(28) Moad, G.; Solomon, D. *The Chemistry of Radical Polymerization*, 2nd fully revised ed.; Elsevier Ltd.: Amsterdam, 2006.
(29) Yoshinobu, Y.; Muhammad, E.; Sato, K.; Goto, A.; Fukuda, T. *Macromolecules* **2001**, *34*, 8872.
(30) (a) Sotzing, G.; Reynolds, J.; Steel, P. *Chem. Mater*. **1996**, *8*, 882–889. (b) Geissler, U.; Hallensleben, M.; Rhode, N. *Synth. Met*. **1997**, *84*, 173–174.
(31) Schrebler, S.; Grez, P.; Cury, P.; Veas, C.; Merino, M.; Gómez, H.; Córdova, R.; del Valle, M. *J. Electroanal. Chem*. **1997**, *430*, 77.
(32) (a) Sarac, A.; Evans, Q.; Serantoni, M.; Clohessy, J.; Cunnane, V. *Surf. Coat. Technol*. **2004**, *182*, 7–13. (b) Ferraris, J.; Haillon, T. *Polymer* **1989**, *30*, 1319. (c) Yassar, A.; Garnier, F. *Macromolecules* **1989**, *22*, 804. (d) Wei, Y.; Chan, C.; Tian, T.; Jang, G.; Hseuh, K. *Chem. Mater*. **1991**, *3*, 888.
(33) Berlin, A. In *Electrical and Optical Polymer Systems - Fundamentals, Methods, and Applications*; Marcel Dekker: New York, 1993; p 47.
(34) Kaneto, K.; Yoshino, K.; Inuishi, Y. *Solid State Commun*. **1983**, *46*, 389–391.
(35) Caspar, J.; Ramamurthy, V.; Corbin, D. *J. Am. Chem. Soc*. **1991**, *113*, 600–610.
(36) Santos, M.; Rubira, A.; Pontes, R.; Basso, A.; Girotto, E. *J. Solid State Chem*. **2006**, *10*, 117–122.
(37) (a) Takolpuckdee, P.; Mars, C.; Perrier, S. *Org. Lett*. **2005**, *7*, 3449–3452. (b) Perrier, S.; Takolpuckdee, P.; Mars, C. *Macromolecules* **2005**, *38*, 6770–6774. (c) Peng, Q.; Lai, D.; Kang, E.; Neoh, K. *Macromolecules* **2006**, *39*, 5577–5582.
(38) (a) Li, C.; Benicewicz, B. *Macromolecules* **2005**, *38*, 5929–5936. (b) Hong, C.; You, Y.; Pan, C. *J. Polym. Sci., Part A: Polym. Chem*. **2006**, *44*, 2419–2427. (c) Li, C.; Han, J.; Ryu, C.; Benicewicz, B. *Macromolecules* **2006**, *39*, 3175–3183.
(39) (a) Buckel, F.; Effenberger, F.; Yan, C.; Golzhauser, A.; Grunze, M. *Adv. Mater*. **2000**, *12*, 901. (b) Fan, L.; Yang, Y.; Tão, Y. *J. Electron Spectrosc. Relat. Phenom*. **2005**, *144*−*147*, 433–436.
(40) Morf, P.; Raimondi, F.; Nothofer, H.; Schnyder, B.; Yasuda, A.; Wessels, J.; Jung, T. *Langmuir* **2006**, *22*, 658–663.
(41) Rieley, H.; Price, N.; Smith, T.; Yang, S. *J. Chem. Soc., Faraday Trans*. **1996**, *92*, 3629.
(42) (a) Duwez, A. S.; Guillet, P.; Colard, C.; Gohy, J. F.; Fustin, C. *Macromolecules* **2006**, *39*, 2729–2731. (b) Bain, C.; Biebuyck, H.; Whitesides, G. M. *J. Am. Chem. Soc*. **1989**, *5*, 723–727. (c) Bourg, M. C.; Badia, A.; Lennox, R. B. *J. Phys. Chem. B* **2000**, *104*, 6562–6567. (d) Castner, D. *Langmuir* **1996**, *12*, 5083–5086.
(43) Tria, M. C.; Grande, C. D.; Ponnapati, R. R.; Advincula, R. *Biomacromolecules* **2010**, *11*, 3422–3431.